



## Article

# Integrating In Situ and Current Generation Satellite Data for Temporal and Spatial Analysis of Harmful Algal Blooms in the Hartbeespoort Dam, Crocodile River Basin, South Africa

Khalid Ali <sup>1,2,\*</sup>, Tamiru Abiye <sup>3</sup> and Elhadi Adam <sup>2</sup> <sup>1</sup> Department of Geology and Environmental Geosciences, College of Charleston, Charleston, SC 29424, USA<sup>2</sup> School of Geography, Archaeology and Environmental Studies, University of the Witwatersrand, Johannesburg 2050, South Africa<sup>3</sup> School of Geosciences, University of the Witwatersrand, Johannesburg 2050, South Africa

\* Correspondence: alika@cofc.edu

**Abstract:** The Hartbeespoort Dam is a discharge point of a catchment that is characterized by urbanization, mining, industrial, and agricultural activities. These activities coupled with fluxes of heavily polluted wastewater from informal settlements, wastewater treatment works, as well as runoff from golf courses have led to the development of recurring harmful algal blooms (HABs). The predominant cyanobacteria scum that is largely covering the Dam water is toxic to fish and poses serious public health risks. Phosphorus is the limiting nutrient in terrestrial aquatic systems and excess concentration in the waters usually results in eutrophication. The productivity level in Hartbeespoort Dam is also a function of total phosphorous (TP) level, showing a positive correlation with chlorophyll-a, an index for phytoplankton which are predominantly HABs in this Dam. Analysis of long-term in situ water quality data (1980–2020) show that TP is not the only driver, changes in surface water temperatures also affect the productivity level, especially, when TP levels are below a threshold of approximately 0.4 mg/L. Chlorophyll-a was retrieved from current generation high resolution satellite (Landsat and Sentinel) at 5-year interval. Standard band ratio-based ocean color model applied to satellite data produced an accuracy of  $R^2 = 0.86$  and RMSE of 5.56  $\mu\text{g/L}$ . Time series analysis of in situ and satellite data show similar trends including capturing the effect of biocontrol on productivity levels between the late 1980s and the early 1990s, after which productivity increased with an increased flux of TP. Since 2015, the average annual surface temperature in the Dam has decreased leading to the decline in productivity level despite increasing levels of TP. The spatial dynamics of the HABs is a function of the discharges levels of the various rivers draining into the Dam as well as its geometry. Relatively higher concentrations are observed near river discharges and in areas of restricted water circulation.

**Keywords:** cyanobacteria; chlorophyll-a; water quality; HABs; remote sensing; Hartbeespoort Dam

**Citation:** Ali, K.; Abiye, T.; Adam, E. Integrating In Situ and Current Generation Satellite Data for Temporal and Spatial Analysis of Harmful Algal Blooms in the Hartbeespoort Dam, Crocodile River Basin, South Africa. *Remote Sens.* **2022**, *14*, 4277. <https://doi.org/10.3390/rs14174277>

Academic Editor: Raphael M. Kudela

Received: 15 July 2022

Accepted: 23 August 2022

Published: 30 August 2022

**Publisher's Note:** MDPI stays neutral with regard to jurisdictional claims in published maps and institutional affiliations.



**Copyright:** © 2022 by the authors. Licensee MDPI, Basel, Switzerland. This article is an open access article distributed under the terms and conditions of the Creative Commons Attribution (CC BY) license (<https://creativecommons.org/licenses/by/4.0/>).

## 1. Introduction

Climate change, urbanization, and agricultural activities have negative environmental impacts on freshwater bodies adding stress on the already scarce resource, especially, in developing countries such as South Africa. Currently, 68% of South Africa's population lives in urban areas, and this is expected to increase to 71% by 2030 (PMG, 2021; <https://pmg.org.za/page/Urbanisation>, accessed on 6 June 2022). Based on the current trend, it is also likely that the majority of future urban growth will be in informal areas as governments struggle to keep up with the increasing demand for basic services including water supply, sanitation, and formal housing. Such kinds of informal settlements are directly linked to the degradation of environmental quality, including water quality [1]. Runoff from agricultural land or other land uses with high application of fertilizers can also further exacerbate the water quality issue. As part of positive feedback process,

deterioration in water quality can have significant economic impacts on the communities dependent on the streams, rivers, lakes, or other open freshwater bodies both for direct use, but also indirectly in terms of the water-dependent economic activities such as fishing [2].

Most of the reservoirs and impoundments in South Africa are located downstream of densely populated urban areas, thereby becoming nutrient enriched as a result of receiving untreated wastewater, raw sewage, and agricultural runoff [3]. Enrichment of nutrients, particularly total phosphorus (TP), which is the limiting nutrient in freshwater bodies, leads to eutrophication [2,4–6]. Studies of eutrophication in aquatic ecosystems has been extensively studied [7–9]; however, the significance of its impacts in South Africa has only recently been realized [10–13].

The Hartbeespoort Dam is a 195 million cubic meters reservoir with an average depth 10 m and is primarily used for irrigation and recreational activities. The reservoir is one of the highly productive eutrophic systems in the Gauteng Province of South Africa (Figure 1). It receives input from streams and rivers that drain the Johannesburg region (formal and informal settlements), industrial developments, agricultural activities, and golf courses. It also receives a significant amount of treated and partially treated water from Waste Water Treatment works (WWTW) at a rate of 5000 L/s [14,15]. Moreover, the poor performance of WWTW, the wide spread agricultural activities, and the lack of compliance monitoring in South Africa's water resources have triggered numerous discharges of inadequately treated wastewater effluents, industrial, and agricultural effluents into the country's already threatened water resources [16].

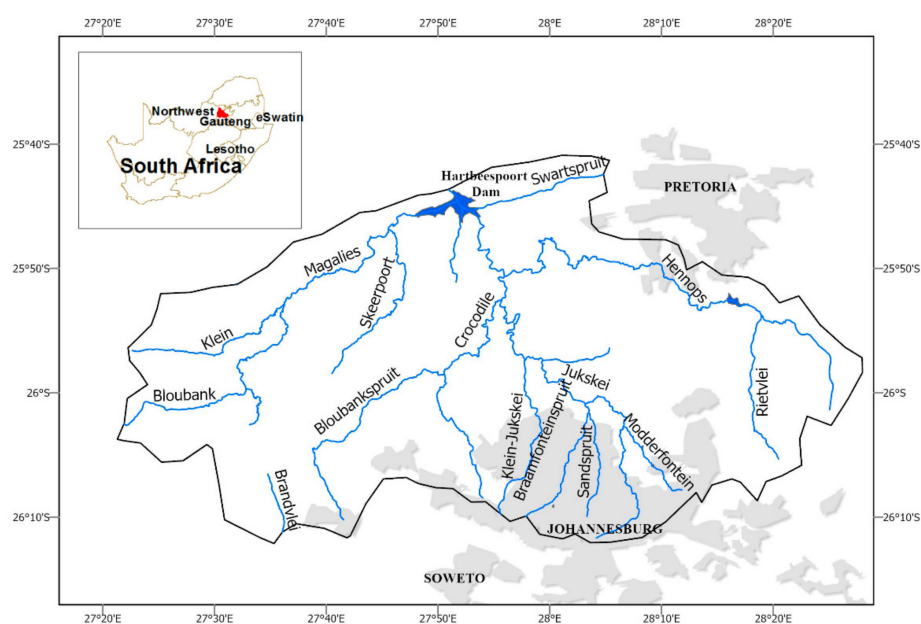


**Figure 1.** Map of the Hartbeespoort Dam and its watershed with drainage system indicated by lines.

These activities have led to the development of recurring algal blooms that are dominated by *Microcystis aeruginosa* characterized as harmful algal blooms (HABs) and the growth of invasive floating aquatic macrophyte, hyacinth [17–20]. Hartbeespoort Dam has been known for the occurrence of massive blooms, mostly exceeding the 20 µg/L chlorophyll-a cut-off trophic state level, of the potentially toxin producing cyanobacterium [21–25]. The cyanobacterial scum that is largely covering the Dam water is toxic to fish and poses serious public health risks [19,20,23].

Distributions of HABs in space and time have major implications for water quality and ecosystem function [2,23,26]. Water resource managers require robust water quality monitoring that is critical to address the question of how various natural and anthropogenic factors affect the health of these environments and to characterize the onset and the temporal and spatial scale of HABs. Currently, water quality assessment is based on in situ

sampling and observation in the Hartbeespoort Dam at select locations. However, in-situ sampling, monitoring, and assessment of water quality require significant logistical and financial resources, which many developing countries such as South Africa lack. These kinds of conventional approaches of observation are challenging for large Dam water systems, where productivity levels change spatially and temporally. A remote sensing approach overcomes some of these challenges by providing a synoptic view of the aquatic bodies at high spatial and temporal resolution, with the potential to greatly improve our understanding of water quality variations. This method also allows for effective water quality monitoring, particularly in surveillance programs of HABs and provides researchers high resolution data for ecological and climate-related studies [7,27].

Current generation satellites have high spectral and radiometric resolution sensors that can detect variations in reflectance from open water surfaces [7,8,28,29]. Measured reflectance at multiple spectral windows carry spectral signatures that characterize various water quality parameters (WQP) such as chlorophyll-a and turbidity [30–33]. Chlorophyll-a, a universal pigment that is used as an index for phytoplankton or HABs, is an optically active constituent that alters irradiance light through absorption and scattering and changes the spectral signature of reflected radiance from water bodies [31,34]. These return signatures in the portion of visible and near-infrared bands of the electromagnetic spectrum are used to model chlorophyll-a concentration in the water body.

Several ocean color (OC) algorithms have been developed to retrieve concentrations of biochemical constituents in the upper euphotic zone using the reflectance from the water column. These algorithms relate measurements of satellite remote sensing reflectance  $R_{rs}(\lambda)$  to chlorophyll-a to provide e.g., phytoplankton biomass approximation [34–36].

In waters dominated by phytoplankton (Case I waters), blue and green wavelength-based OC algorithms have been successfully used to retrieve chlorophyll-a concentrations [7,37]. In coastal and inland waters (Case II waters), multiple biochemical constituents affect remote sensing reflectance,  $R_{rs}(\lambda)$ , including suspended sediments, tripton, and the presence of HABs [8,26,38–40]. The various in-water constituents competing absorb light in the blue spectral region and may add to uncertainties when using this region to detect specifically chlorophyll-a concentration [34,41–43]. The  $R_{rs}$  products have been evaluated in Case-2 waters using data from the Aerosol Robotic Network (AERONET-OC) and showed that the red-infrared band combinations can be effective for the  $R_{rs}$  based retrievals in optically complex (Case II) turbid waters [44]. In the recent study carried out by [11], in a nearby reservoir, the Vaal Dam, it was demonstrated that both the blue-green and red-infrared based OC chlorophyll-a algorithms worked effectively when applied to high resolution sensors. This may be attributed to the overwhelmingly strong signal from the excessively high chlorophyll-a concentrations in the water column, which is also the case in the Hartbeespoort Dam.

Current generation satellite sensors such as the Landsat 8 OLI and Sentinel 2 MSI are equipped with spectral windows that are sensitive to chlorophyll-a's absorption features. These sensors have relatively high spatio-temporal and radiometric resolution and therefore, allow for better spatial characterization of the water quality dynamics in large open waters bodies such as the Hartbeespoort Dam [11,28,37,39].

Application of satellite remote sensing to monitor water quality of large open waters in South Africa is primitive. The aim of the study is to evaluate long-term water quality changes in the Hartbeespoort Dam using an integrated approach of in situ data and multispectral satellite sensors. Specific goals of this study are to (a) evaluate long-term (1980–2021) nutrient loading into the Dam and the response in productivity, and (b) apply Landsat 8 OLI and Sentinel 2 MSI for spatio-temporal assessment of HABs, using chlorophyll-a as an index. For the satellite-based chlorophyll-a retrievals, we focused on satellite data that were collected in late summer, when productivity is at peak level, and the signal-to-noise ratio is high.

## 2. Study Area

The Hartbeespoort Dam is the outflow of the Upper Crocodile River Basin (UCRB) (Figure 1), which constitutes part of the Crocodile West and Marico Water Management Area as per the Department of Water and Sanitation (DWS) classification. The basin covers an area of approximately 6300 km<sup>2</sup> [12] within the Gauteng and North West Provinces of South Africa. Due to the presence of high topography in the south of the basin, the UCRB is generally drained in a northerly direction. The confluence of the Jukskei and Hennops rivers in the east of the basin produces the Crocodile River, which contributes to 90% of Hartbeespoort Dam's inflow [15]. The Magalies River flowing from the west contributes minor inflow to Hartbeespoort Dam. The Crocodile River flows northward from Hartbeespoort Dam into the Limpopo river.

The UCRB is characterized by a subtropical highland climate with a mean annual rainfall of 700 mm [45]. The basin generally receives most of the rainfall between the summer months of October and March, which occurs as convective rainfall in the form of afternoon thundershowers and occasional hailstorms [46,47]. The average temperatures in summer are a minimum of 15 °C and a maximum of 30 °C while winter temperatures range from 5 °C to 25 °C [48].

## 3. Materials and Methods

### 3.1. Water Quality Data

Water quality data were obtained from the water management system database of the Department of Water and Sanitation (DWS) in South Africa. The DWS maintains water quality data throughout the UCRB watershed including on sites within the Hartbeespoort Dam. Data are available since 1980 although a gap exists between 1983 and 1987. The data include major ion chemistry, total phosphorus concentrations (TP), and chlorophyll-a concentrations. Physical data include in situ temperature and dissolved oxygen (DO) measurements taken at multiple depths.

Time-series graphs for temperature (°C), DO concentrations (mg/L), TP concentrations (mg/L), and chlorophyll-a concentrations (µg/L) are plotted. Annual-based trend analysis is run on the time series data and a line plot is added to each time series to assess long-term changes of the parameters. Trend analyses were also run to show decadal changes using a 5 m depth integrated temperature, DO concentrations (mg/L), TP concentrations (mg/L), and chlorophyll-a concentrations (µg/L). The correlation between these parameters has also been evaluated.

### 3.2. Satellite Data

Level 2 Landsat OLI and Sentinel 2 MSI satellite data of the study area are acquired from USGS earth explorer <https://earthexplorer.usgs.gov/>, accessed on 5 May 2022) and Copernicus Open Access Hub (<https://scihub.copernicus.eu/dhus/#/home>, accessed on 5 May 2022, respectively. Data were acquired for the month of April at five-year intervals, as available between 1980 and 2020. This allows for understanding long-term changes without much influence from short-term effects including annual and inter-annual seasonal anomalies. We specifically focused on satellite data from late summer (April) as a period of reference, where chlorophyll-a and bloom events are at peak level. Landsat 5/7 data were obtained for the period 1995 to 2010. Both series have near identical sensor characteristics in-terms of resolution and band placements. For recent dates (2013 onwards) the Landsat 8 and Sentinel 2 data were used. Both have higher radiometric resolution of 12 bit which allows for the enhanced capability to discriminate very slight differences in the water column optics which is a function of WQPs. The new generation sensors are also equipped with more spectral bands that are narrower creating the opportunity to identify specific materials by their band absorption characteristics. The Sentinel 2 sensor has a higher spatial resolution of 10 m than the Landsat series (30 m).

NASA's standard ocean color processing software the SeaWiFS Data Analysis System (SEADAS; version 8) level -2 generator (l2 gen) is used to process the images, perform the

atmospheric correction process, and retrieve remote sensing reflectance ( $R_{rs}$ ) per unit steradian ( $sr$ ) and the normalized water-leaving radiance ( $nLw$ ) [49,50]. For this analysis, the multi-scattering with 2-band model selection and iterative near infra-red (NIR) correction method is applied [51]. This method is effective in turbid waters and attempts to separate the radiometric signal of suspended particulates from aerosol noise [52–56]. Cloud free images were downloaded but additional cloud masks are applied to remove haze related effects using the standard SeaDAS masking default thresholds from the NIR spectral region. A land mask was also applied to remove the land component and retrieve images of the open water body only.

Spectral band ratios are applied to both Sentinel and Landsat satellite images for modeling productivity levels of the Dam water. This study uses two standard OC chlorophyll-a retrieval models, specifically the two-band blue-green-based algorithm as presented in [36] or the NIR-red model given by [33] depending on performances. These ratio-based models are expressed as:

$$Chl\ a \approx \frac{R_{(\lambda_1)}^1}{R_{(\lambda_2)}^1} \quad (1)$$

The models are based on ratios of spectral regions that are sensitive to absorption and scattering features of chlorophyll-a. The spectral regions are matched with the corresponding satellites bands. The chlorophyll-a concentrations retrieved using the two-band models are used to present the spatial and temporal dynamics of the HABs.

#### 4. Result and Discussion

Distribution analysis of biophysical parameters between 1980 and 2020 shows that concentration levels of chlorophyll-a in the Hartbeespoort Dam varied from approximately 3.5  $\mu\text{g/L}$  to 390  $\mu\text{g/L}$ , and TP levels ranged from 0.1 mg/L to 1.5 mg/L (Figure 2). During the same period, average temperature and DO were approximately 19  $^\circ\text{C}$  and 8.4 mg/L, respectively. The chlorophyll-a data is positively skewed with mean centered near the low range values. Figure 2 shows that for chlorophyll-a, 75% of the data fall below the 55  $\mu\text{g/L}$  level. This trend is also observed in the TP values where the values range from 0–1.5 mg/L with the mean centered around 0.4 mg/L. Temperature and DO data have values that follow a relatively normal distribution with few outliers on both sides. The extremely low frequency outliers in temperature and DO may be attributed to systematic or random errors.

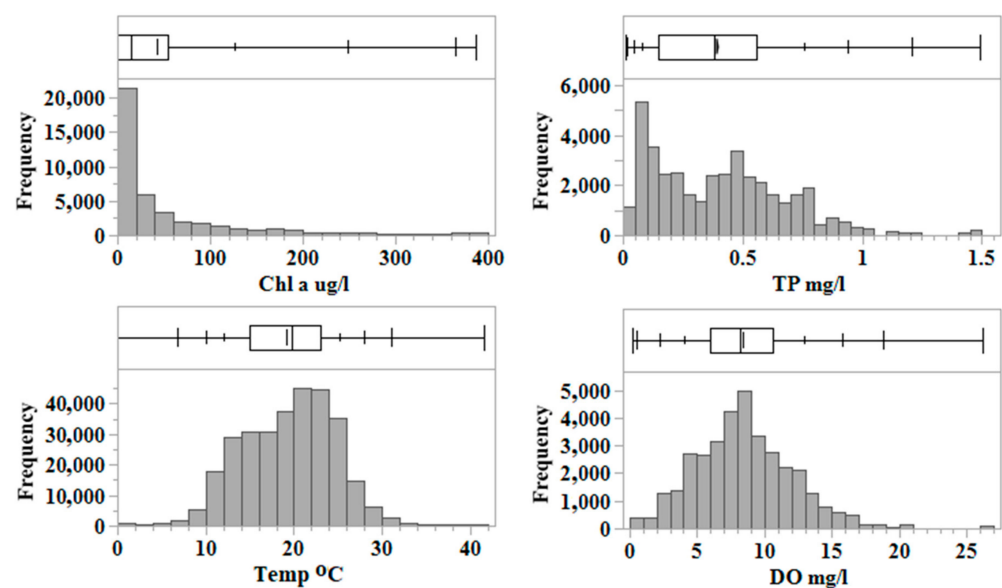
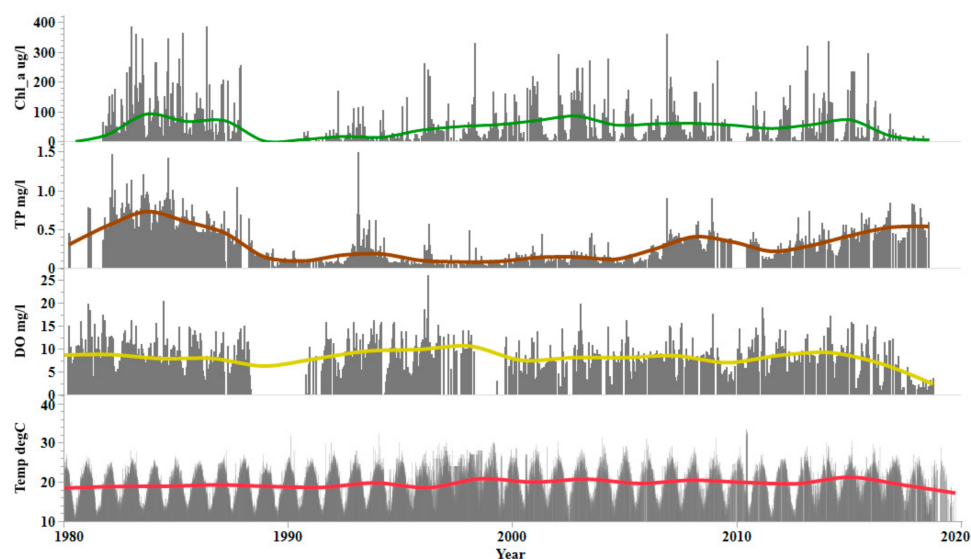


Figure 2. Distribution plot of various water quality parameters in the Hartbeespoort Dam; DWS.

Time series plot of chlorophyll-a, TP, DO, and temperature show seasonal, annual, and decadal variation of the water quality parameters (Figure 3). Concentrations of the TP nutrient were high between 1982 and 1986 with values consistently greater than 0.5 mg/L and reaching up to 1.5 mg/L. The chlorophyll-a was also high with an average concentration of 52  $\mu\text{g/L}$ . These values put the waters in the hypereutrophic status [57]. TP values decreased significantly by the late 1980s and into the early 1990s, primarily in response to the bioremediation project [18]. Chlorophyll-a concentration in the Hartbeespoort Dam also decreased during the 1990s, and the average value dropped to 20  $\mu\text{g/L}$ . However, when biocontrol project ended in late 1990s, due to lack of funding, chlorophyll-a concentrations spiked in the 2000s reaching values near 400  $\mu\text{g/L}$  with an average of 64  $\mu\text{g/L}$  between 2000 and 2010. In the past decade (2010–2018), there was a general decrease in productivity in the Dam but the average chlorophyll-a remained high at 45  $\mu\text{g/L}$ , which is well above the 7  $\mu\text{g/L}$  threshold for eutrophic systems (Figure 3) [25]. Although the amount of TP concentration continues to increase, a steep decline in the chlorophyll-a concentrations has been observed since 2015. This also correlates with drop in temperature during the same period (Figure 3). This indicates that temperature has strong influence on productivity and DO levels. Higher chlorophyll-a and DO values correspond to warmer seasons and vice-versa. The increase in TP over the past two decades can be linked to higher discharges of untreated wastewater along with other anthropogenic nutrient sources such as agricultural and golf course runoffs.



**Figure 3.** Time series of water quality parameters in the Hartbeespoort Dam; DWS.

Over the long-term (past 4 decades), temperature and DO show near constant values with a sharp decline in 2015 (Figure 3). Chlorophyll-a follows the 2015 declining trend while TP levels continue to rise. To understand these relationships at higher resolution, the data were categorized by decades. During the period from 1980 to 1990; chlorophyll-a, TP, and DO showed a decline while temperature increased by 0.8  $^{\circ}\text{C}$  (Figure 4a). The average annual concentration of chlorophyll-a decreased from  $\sim 62$   $\mu\text{g/L}$  to  $\sim 40$   $\mu\text{g/L}$ ; the average DO levels changed from  $\sim 9.1$  mg/L to 7.5 mg/L and the TP levels dropped from an average of 0.7 mg/L to 0.2 mg/L. The decline of TP and chlorophyll-a overlaps with the implementation period (late 1980s to the early 1990s) of the bioremediation project which ultimately reduced the chlorophyll-a levels by up to 80% [18]. The increase in measured temperature records during this decade could be attributed to the dominance of the El Niño effect over La Niña where the years 1982 and 1983 were characterized by drought throughout the country [58]. The effect of continued bioremediation into the 1990's is reflected in the further decline of TP levels between 1990 and 2000 (Figure 4b). However, during the same period, chlorophyll-a increased significantly to levels of up to 60  $\mu\text{g/L}$

causing super-saturation in DO and reaching 11 mg/L. The increase in productivity may be attributed to the sudden increase in loading of TP into the Dam as recorded between 1992 and 1995 (Figure 4b). During this decade the Dam was also going through temperature stabilization. This shift in temperature trend could be linked to the weakening of the El Nino effect in the region leading to cooler temperatures over the decade (Figure 4b).

In the past two decades (2000–2020), as the result of increased urbanization and increased flux of untreated or partially treated wastewater, TP levels in the Hartbeespoort Dam have been significantly increasing (Figure 4c,d). However, despite this increase in TP concentrations of the limiting nutrient, the average chlorophyll-a and DO levels have been decreasing at a rate of up to 7.5  $\mu\text{g/L/year}$  and 0.8 mg/L/year, respectively (Figure 4c,d). The biocontrol project kept TP levels relatively low between 1990 and 2010 compared to the 1980s where levels were consistently higher at TP > 0.7 mg/L. However, recent records of TP levels are approaching to that of the 1980s. A slightly higher average surface water temperature was recorded during the past two decades but inter-annual variability over the 10 year periods shows a decreasing trend by as much as 1.5  $^{\circ}\text{C}$  or at a rate of 0.15  $^{\circ}\text{C/year}$  (Figure 4c,d). This temperature gradient could be due to the El Nino effect that affected South Africa in 2015 and 2016 [58].

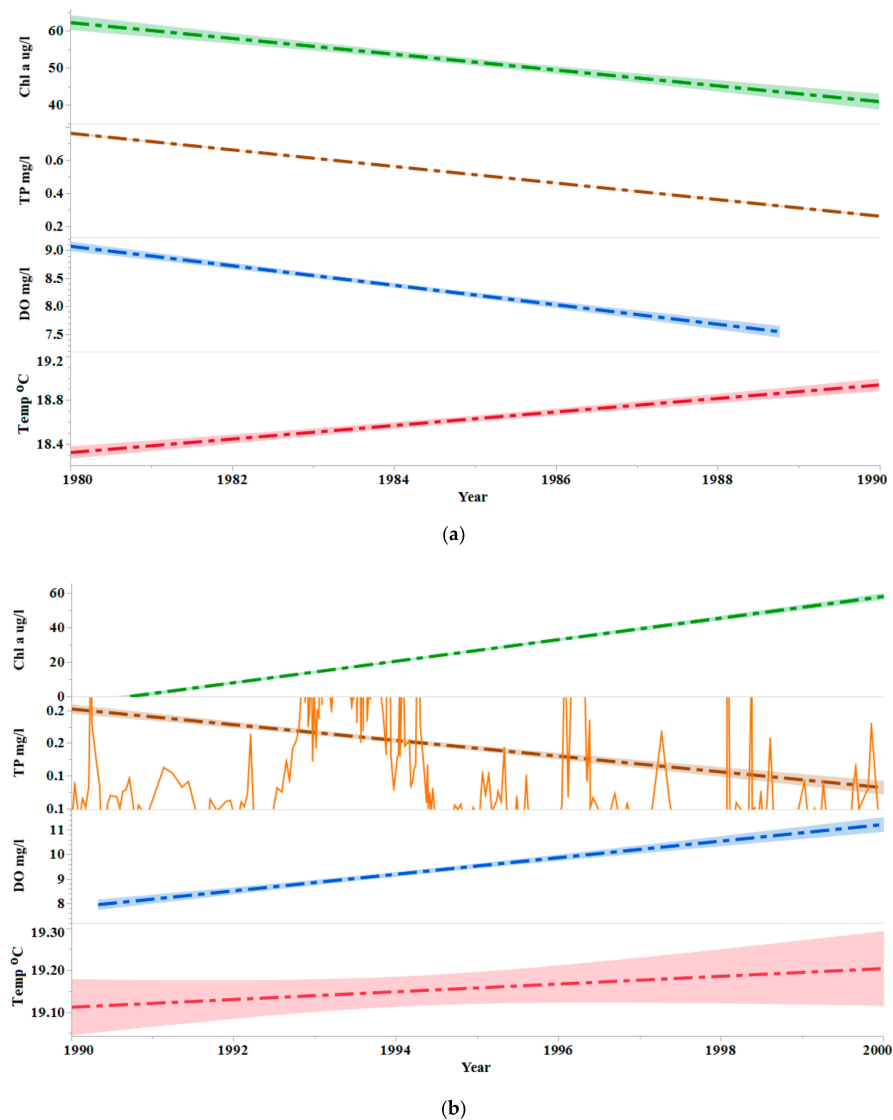
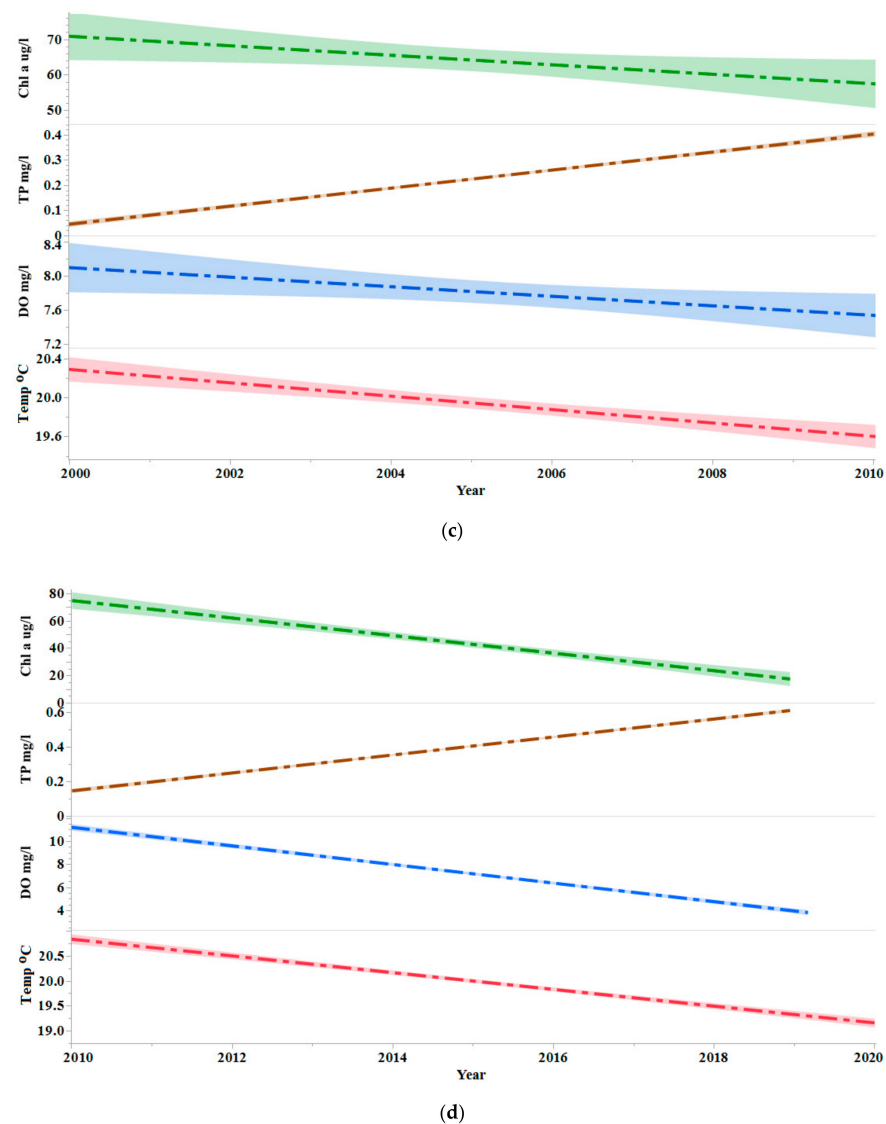


Figure 4. Cont.



**Figure 4.** Decadal trends of chlorophyll-a, TP, DO and temperature in the Dam during (a) 1980–1990, (b) 1990–2000, (c) 2000–2010, (d) 2000–2010; DWS.

Productivity in the open water system is a function of multiple biophysical factors but limiting nutrients such as TP are considered the major drivers in many aquatic settings [12,13,18,31,59]. However, results in this study have shown that TP is not necessarily the only factor driving phytoplankton growth in the Hartbeespoort Dam. This is especially the case when TP levels are relatively low, in this case below 0.4 mg/L. Chlorophyll-a concentration in Hartbeespoort Dam showed a decreasing trend for the past two decades while the TP levels were increasing. The steep decline in the temperature slope, chlorophyll-a and DO as shown in Figures 3 and 4c,d clearly indicate that temperature plays a significant role in controlling productivity in the Hartbeespoort Dam. The effect of temperature on productivity is well documented in previous studies [60,61].

The regression analysis between the water quality parameters shows a positive correlation between chlorophyll-a and temperature; chlorophyll-a and DO; chlorophyll-a and TP; as well as between temperature and DO (Figure 5). The data between 1980 and 1990 showed productivity in the Dam was primarily influenced by TP when concentrations were high. But in recent decades, despite the increase in TP, chlorophyll-a has continued to decrease. As temperature changes, the productivity in the Dam also changes which in turn affects the net DO levels. The TP's positive correlation with chlorophyll-a indicates the



effect of nutrient loading in the Dam, however, the near zero correlation with the physical parameters such as the DO suggests that TP may not necessarily be the main driver of the productivity in the Dam. These relationships confirm temperature as the main driver of the biophysical dynamics in the Dam's aquatic system. Our study shows that a TP level of above 0.4 mg/L is required to drive the primary productivity. However, these effects require further study.

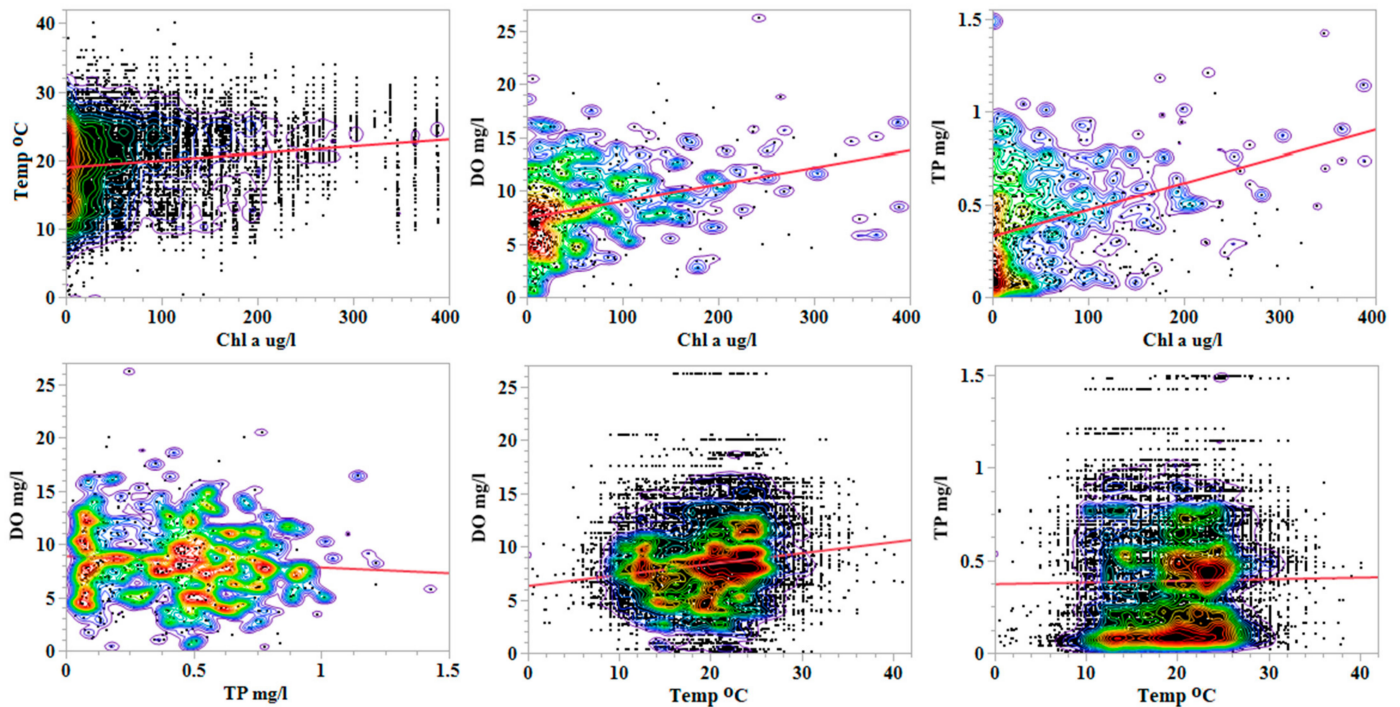


Figure 5. Scatter plots between the various water quality parameters; DWS.

Regression analysis between satellite-based and in-situ chlorophyll-a data show a strong correlation with an  $R^2 = 0.86$  and RMSE of  $5.56 \mu\text{g/L}$  (Figure 6). This demonstrates the applicability of global OC model to effectively retrieve chlorophyll-a in large productive open waters such as the Hartbeespoort Dam, where productivity levels are high. The OC model was used to predict chlorophyll-a level for 2020, where in situ data are not available.

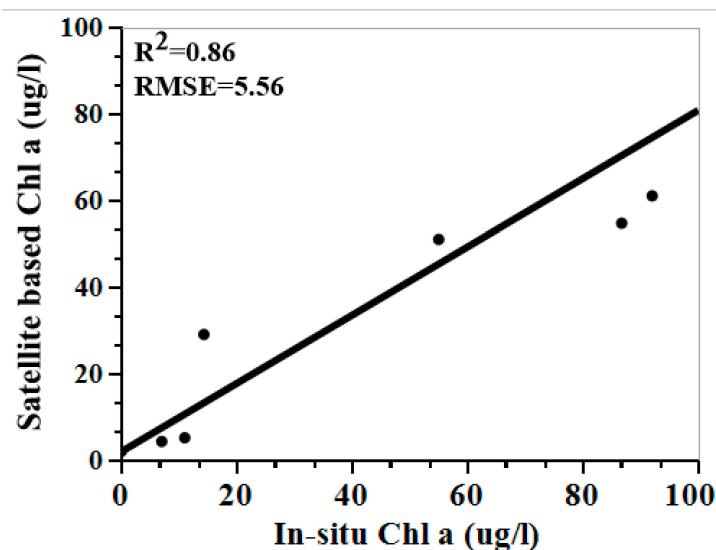
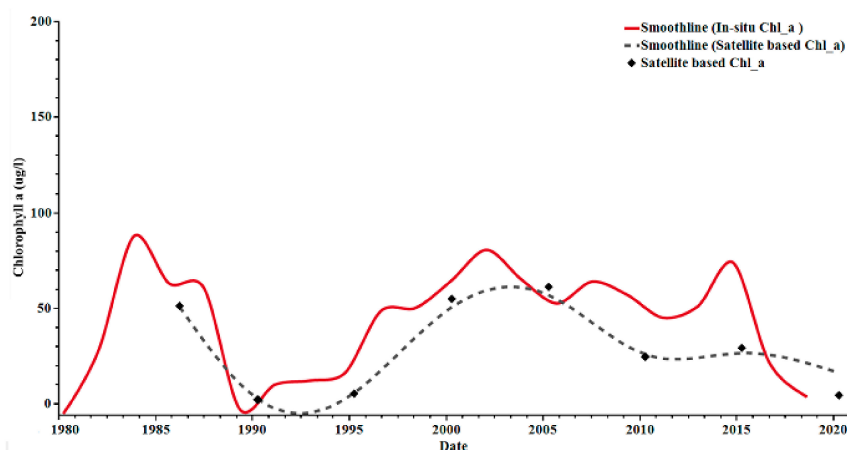


Figure 6. Satellite chlorophyll-a estimates comparisons against in-situ concentrations.

Time series plots of the 5-year interval satellite-based and the in situ chlorophyll-a data show the interdecadal variability of productivity levels in the Hartbeespoort Dam (Figure 7). The satellite data captures the major shifts in chlorophyll-a concentrations in the Dam. The steep decline in the satellite-based chlorophyll-a level during mid-to-late 1980s, and the continuous low chlorophyll-a level in the early 1990s reflects the effects of the bioremediation project. Satellite data also captured the increase in productivity level between the mid-1990s and early-2000s, which is attributed to increased urbanization and higher discharges of untreated wastewater along with other anthropogenic sources. The general decline in satellite-based chlorophyll-a levels between mid-2000 and 2015 mimics the observed in situ chlorophyll-a trend. As of 2015, there is a steep decline in the chlorophyll-a concentrations which is also captured by the satellite data.



**Figure 7.** Time series of chlorophyll-a data retrieved from satellite and in-situ measurements.

The spatial and temporal changes of water quality and the dynamics of the HABs across the Hartbeespoort Dam is shown in Figure 8. The Landsat series data are primarily used because of its large temporal coverage and was supplemented with Sentinel 2 data for the recent years. In this study, a five-year interval satellite data were used to understand the long-term spatial and temporal dynamics of HABs in the reservoir by consistently comparing images from April (late summer), as a period of reference, where productivity levels are considered to be at maximum levels. This interval of data collection also minimized influence of annual and seasonal changes. A total 20 satellite images were processed and normalized to be able to compare the variation over time. The image that was taken in 1985 (Figure 8a) shows relatively high concentration levels of chlorophyll-a which is linked to high TP levels in the system (Figure 3). Relatively higher productivity is observed near the discharge areas of the crocodile river as well as near the western part of the dam where the Magalis river is discharged (Figure 8b). The relatively high level in the western parts could be attributed to direct runoff from golf courses and restricted water circulation in the reservoir.

The positive impact of bioremediation in the late 1980s can be visualized in the image taken in April of 1990, where productivity level was significantly low (Figure 8c,d). Since the bioremediation project took place in the early 1990s, productivity levels also remained relatively low in mid-1990s as shown in Figure 8e,f. This is consistent with the measured ground data as presented in Figure 3. With the end of the biocontrol measures coupled with an increase in TP levels, productivity in the reservoir increased between the late 1990s and the early 2010s (Figure 8g,h). The five-year interval images between 2000 and 2010 show a progressive increase in phytoplankton biomass (Figure 8i–l). This is also the period where TP levels started to increase due to increased human activities such as discharges of untreated or partially treated wastewater, runoff from urban areas, agricultural activities, and golf courses. Landsat data from 2015 onwards, and Sentinel 2 data for the past 2 years show a declining trend in the productivity in the Hartbeespoort Dam (Figure 8m–t). These

changes are strongly correlated with the measured in-situ chlorophyll-a and DO levels. The spatial dynamics of the HABs is linked to fluxes of the various rivers draining into the Dam and its geometry.

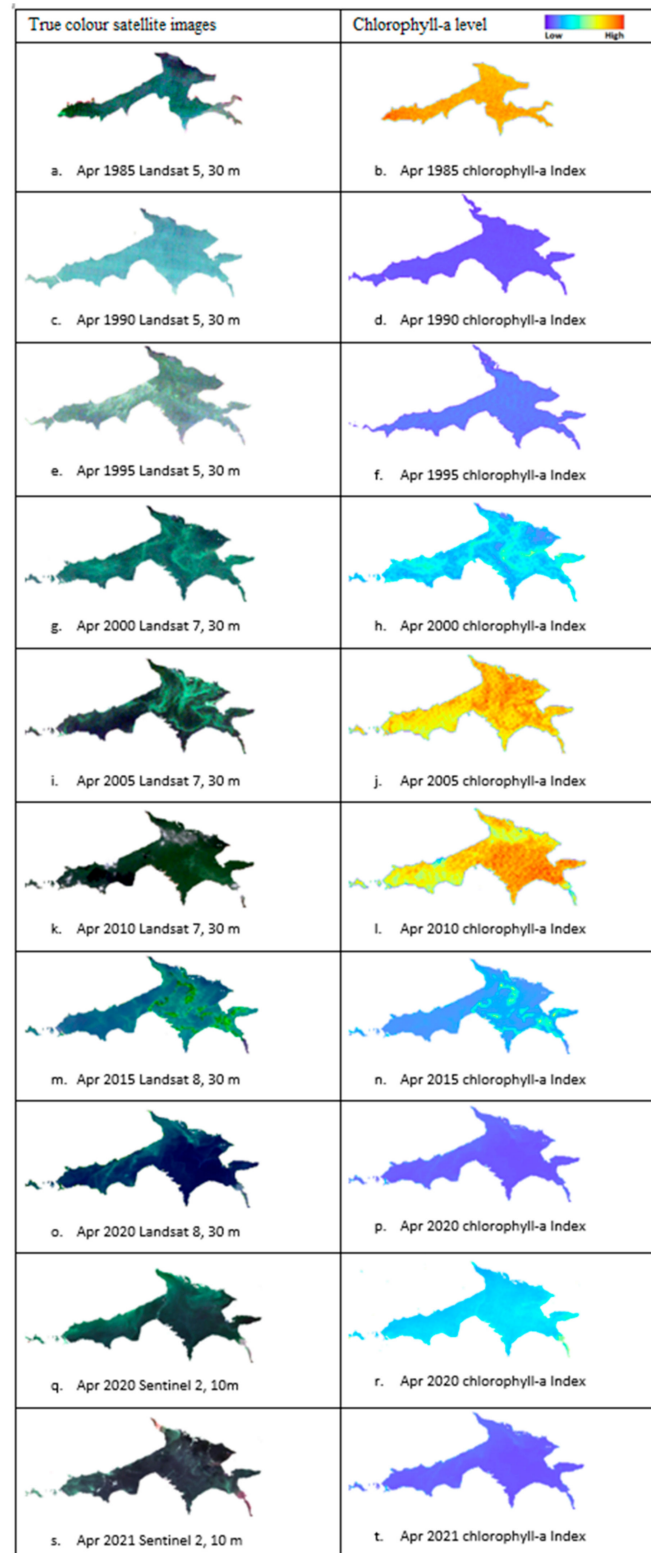


**Figure 8.** Chlorophyll-a concentrations in the Hartbeespoort Dam between 1980–2021 from Landsat and Sentinel.

## 5. Conclusions

The results obtained from the measured temporal water quality data revealed a high level of anthropogenic impact on the Hartbeespoort Dam which was designed to provide water for agricultural and recreational uses. The deterioration of the water quality over the years is exacerbated by the discharge of poor quality and nutrient-rich effluent of untreated wastewater, raw sewage, and agricultural runoff.

The study showed that the productivity levels in the Hartbeespoort Dam is primarily a function of TP levels showing relatively strong positive correlation with chlorophyll-a, an index for phytoplankton and in this case predominantly HABs. This finding is consistent with other studies that showed phosphorous is the limiting factor in freshwater bodies [4–6]. However, in this case, the analysis of long-term in situ water quality data showed that TP is not the only driver. Changes in surface water temperatures also affect the productivity levels, especially, when TP levels are below a threshold of approximately 0.4 mg/L. Since 2015, the average annual surface temperature in the Dam has decreased leading to the decline in productivity levels despite increasing levels of TP.

Chlorophyll-a retrieved from satellite images show the dynamics of HABs over the past four decades. The OC model applied to retrieve the chlorophyll-a in the Hartbeespoort Dam performed at an accuracy of  $R^2 = 0.86$ , RMSE = 5.56  $\mu\text{g/L}$ . Relatively high chlorophyll-a concentrations were observed at river discharge points near the reservoir mouth, and in peripheral regions where nutrient rich waters runoff and water circulations are restricted due to low levels of mixing. Time series analysis of the 5-year interval satellite data captured the major shifts and trends of chlorophyll-a levels in the Dam. The data has showed the positive effect of biocontrol on productivity level between the late 1980s and the early 1990s. However, when biocontrol was terminated in mid-1990s, productivity increased with an increased flux of TP from uncontrolled disposal of wastewater. The bioremediation activity of the late 1980s and early 1990s was effective in reducing the TP and hence the eutrophication level of the reservoir. The effect of declining surface water temperature since 2015 on productivity levels is also evident from the satellite data showing decrease in productivity both spatially and temporally. This is consistent with the dynamics observed in measured data. Further studies will be conducted to understand short-term effects including annual, inter-annual, and seasonal changes in HAB dynamics.

**Author Contributions:** Conceptualization, K.A., E.A. and T.A.; Formal analysis, K.A.; Funding acquisition, E.A.; Investigation, K.A.; Methodology, K.A.; Writing—original draft, K.A.; Writing—review & editing, K.A., E.A. and T.A. All authors have read and agreed to the published version of the manuscript.

**Funding:** This research received no external funding.

**Conflicts of Interest:** The authors declare no conflict of interest.

## References

1. Cullis, J.D.S.; Horn, A.; Rossouw, N.; Fisher-Jeffes, L.; Kunneke, M.M.; Hoffman, W. Urbanisation, climate change and its impact on water quality and economic risks in a water scarce and rapidly urbanising catchment: Case study of the Berg River Catchment. *H2Open J.* **2019**, *2*, 146–167. [[CrossRef](#)]
2. Alprol, A.E.; Heneash, A.M.M.; Soliman, A.M.; Ashour, M.; Alsanie, W.F.; Gaber, A.; Mansour, A.T. Assessment of water quality, eutrophication, and zooplankton community in lake Burullus, Egypt. *Diversity* **2021**, *13*, 268. [[CrossRef](#)]
3. Edokpayi, J.N.; Odiyo, J.O.; Durowoju, O.S. Impact of Wastewater on Surface Water Quality in Developing Countries: A Case Study of South Africa. In *Water Quality*; InTech: London, UK, 2017.
4. Blomqvist, S.; Gunnars, A.; Elmgren, R. Why the limiting nutrient differs between temperate coastal seas and freshwater lakes: A matter of salt. *Limnol. Oceanogr.* **2004**, *49*, 2236–2241. [[CrossRef](#)]
5. Cha, Y.K.; Alameddine, I.; Qian, S.S.; Stow, C.A. A cross-scale view of N and P limitation using a Bayesian hierarchical model. *Limnol. Oceanogr.* **2016**, *61*, 2276–2285. [[CrossRef](#)]
6. Elser, J.J.; Bracken, M.E.S.; Cleland, E.E.; Gruner, D.S.; Harpole, W.S.; Hillebrand, H.; Ngai, J.T.; Seabloom, E.W.; Shurin, J.B.; Smith, J.E. Global analysis of nitrogen and phosphorus limitation of primary producers in freshwater, marine and terrestrial ecosystems. *Ecol. Lett.* **2007**, *10*, 1135–1142. [[CrossRef](#)]

7. Ali, K.A.; Ortiz, J.; Bonini, N.; Shuman, M.; Sydow, C. Application of Aqua MODIS sensor data for estimating chlorophyll a in the turbid Case 2 waters of Lake Erie using bio-optical models. *GISci. Remote Sens.* **2016**, *53*, 483–505. [[CrossRef](#)]
8. Ali, K.; Witter, D.; Ortiz, J. Application of empirical and semi-analytical algorithms to MERIS data for estimating chlorophyll a in Case 2 waters of Lake Erie. *Environ. Earth Sci.* **2014**, *71*, 4209–4220. [[CrossRef](#)]
9. Drobac, D.; Tokodi, N.; Simeunović, J.; Baltić, V.; Stanić, D.; Svirčev, Z. Human exposure to cyanotoxins and their effects on health. *Arh. Hig. Rada Toksikol.* **2013**, *64*, 305–316. [[CrossRef](#)]
10. Coetzee, J.A.; Hill, M.P. The role of eutrophication in the biological control of water hyacinth, *Eichhornia crassipes*, in South Africa. *BioControl* **2012**, *57*, 247–261. [[CrossRef](#)]
11. Obaid, A.A.; Ali, K.A.; Abiye, T.A.; Adam, E.M. Assessing the utility of using current generation high-resolution satellites (Sentinel 2 and Landsat 8) to monitor large water supply dam in South Africa. *Remote Sens. Appl. Soc. Environ.* **2021**, *22*, 100521. [[CrossRef](#)]
12. Van Ginkel, C.E.; Silberbauer, M.J. Temporal trends in total phosphorus, temperature, oxygen, chlorophyll a and phytoplankton populations in Hartbeespoort Dam and Roodeplaat Dam, South Africa, between 1980 and 2000. *Afr. J. Aquat. Sci.* **2007**, *32*, 63–70. [[CrossRef](#)]
13. van Ginkel, C.E. Eutrophication: Present reality and future challenges for South Africa. *Water SA* **2011**, *37*, 693–702. [[CrossRef](#)]
14. Leketa, K.C. Holistic Approach to Groundwater Recharge Assessment in the Upper Crocodile River Basin, Johannesburg, South Africa. Ph.D. Thesis, University of the Witwatersrand, Johannesburg, South Africa, 2019.
15. Leketa, K.; Abiye, T.; Butler, M. Characterisation of groundwater recharge conditions and flow mechanisms in bedrock aquifers of the Johannesburg area, South Africa. *Environ. Earth Sci.* **2018**, *77*, 727. [[CrossRef](#)]
16. Naidoo, S.; Olaniran, A.O. Treated wastewater effluent as a source of microbial pollution of surface water resources. *Int. J. Environ. Res. Public Health* **2013**, *11*, 249–270. [[CrossRef](#)]
17. Ashton, P.J.; Robarts, R.D. Apparent predation of *Microcystis aeruginosa* katz. Emend elenkin by a saprospira-like bacterium in a hypertrophic lake (Hartbeespoort Dam, South Africa). *J. Limnol. Soc. S. Afr.* **1987**, *13*, 44–47. [[CrossRef](#)]
18. Auchterlonie, J.; Eden, C.L.; Sheridan, C. The phytoremediation potential of water hyacinth: A case study from Hartbeespoort Dam, South Africa. *S. Afr. J. Chem. Eng.* **2021**, *37*, 31–36. [[CrossRef](#)]
19. Gumbo, R.J.; Ross, G.; Cloete, E.T. Biological control of *Microcystis* dominated harmful algal blooms. *Afr. J. Biotechnol.* **2008**, *7*, 4765–4773.
20. Ballot, A.; Sandvik, M.; Rundberget, T.; Botha, C.J.; Miles, C.O. Diversity of cyanobacteria and cyanotoxins in Hartbeespoort Dam, South Africa. *Mar. Freshw. Res.* **2014**, *65*, 175–189. [[CrossRef](#)]
21. Zohary, T. Hyperscums of the cyanobacterium *Microcystis aeruginosa* in a hypertrophic lake (Hartbeespoort Dam, South Africa). *J. Plankton Res.* **1985**, *7*, 399–409. [[CrossRef](#)]
22. Zohary, T.; Madeira, A.M.P. Structural, physical and chemical characteristics of *Microcystis aeruginosa* hyperscums from a hypertrophic lake. *Freshw. Biol.* **1990**, *23*, 339–352. [[CrossRef](#)]
23. Oberholster, P.J.; Botha, A.M. Use of remote sensing and molecular markers to detect toxic cyanobacterial hyperscum crust: A case study on Lake Hartbeespoort, South Africa. *Afr. J. Biotechnol.* **2010**, *9*, 8783–8790.
24. Conradie, K.R.; Barnard, S. The dynamics of toxic *Microcystis* strains and microcystin production in two hypertrophic South African reservoirs. *Harmful Algae* **2012**, *20*, 1–10. [[CrossRef](#)]
25. Carlson, R.E. A trophic state index for lakes 1. *Limnol. Oceanogr.* **1977**, *22*, 361–369. [[CrossRef](#)]
26. Pahlevan, N.; Smith, B.; Schalles, J.; Binding, C.; Cao, Z.; Ma, R.; Alikas, K.; Kangro, K.; Gurlin, D.; Hà, N. Seamless retrievals of chlorophyll-a from Sentinel-2 (MSI) and Sentinel-3 (OLCI) in inland and coastal waters: A machine-learning approach. *Remote Sens. Environ.* **2020**, *240*, 111604. [[CrossRef](#)]
27. Gurlin, D.; Gitelson, A.A.; Moses, W.J. Remote estimation of chl-a concentration in turbid productive waters—Return to a simple two-band NIR-red model? *Remote Sens. Environ.* **2011**, *115*, 3479–3490. [[CrossRef](#)]
28. Pahlevan, N.; Chittimalli, S.K.; Balasubramanian, S.V.; Vellucci, V. Sentinel-2/Landsat-8 product consistency and implications for monitoring aquatic systems. *Remote Sens. Environ.* **2019**, *220*, 19–29. [[CrossRef](#)]
29. Wu, M.; Zhang, W.; Wang, X.; Luo, D. Application of MODIS satellite data in monitoring water quality parameters of Chaohu Lake in China. *Environ. Monit. Assess.* **2009**, *148*, 255–264. [[CrossRef](#)]
30. Gitelson, A.A.; Dall’Olmo, G.; Moses, W.; Rundquist, D.C.; Barrow, T.; Fisher, T.R.; Gurlin, D.; Holz, J. A simple semi-analytical model for remote estimation of chlorophyll-a in turbid waters: Validation. *Remote Sens. Environ.* **2008**, *112*, 3582–3593. [[CrossRef](#)]
31. Gholizadeh, M.H.; Melesse, A.M.; Reddi, L. A comprehensive review on water quality parameters estimation using remote sensing techniques. *Sensors* **2016**, *16*, 1298. [[CrossRef](#)]
32. Schalles, J.F. Chapter 3 optical remote sensing techniques to estimate phytoplankton chlorophyll a concentrations in coastal waters with varying suspended matter and CDOM concentrations. In *Remote Sensing of Aquatic Coastal Ecosystem Processes*; Springer: Dordrecht, The Netherlands, 2006.
33. Moses, W.J.; Gitelson, A.A.; Berdnikov, S.; Povazhnyy, V. Estimation of chlorophyll-a concentration in case II waters using MODIS and MERIS data—Successes and challenges. *Environ. Res. Lett.* **2009**, *4*, 045005. [[CrossRef](#)]
34. Franz, B.A.; Bailey, S.W.; Kuring, N. Ocean Color Measurements from Landsat-8 OLI using SeaDAS. 2014. Available online: [https://www.researchgate.net/publication/267679321\\_Ocean\\_Color\\_Measurements\\_from\\_Landsat-8\\_OLI\\_using\\_SeaDAS](https://www.researchgate.net/publication/267679321_Ocean_Color_Measurements_from_Landsat-8_OLI_using_SeaDAS) (accessed on 14 July 2022).

35. Binding, C.E.; Greenberg, T.A.; McCullough, G.; Watson, S.B.; Page, E. An analysis of satellite-derived chlorophyll and algal bloom indices on Lake Winnipeg. *J. Great Lakes Res.* **2018**, *44*, 436–446. [[CrossRef](#)]
36. O'Reilly, J.E.; Werdell, P.J. Chlorophyll algorithms for ocean color sensors—OC4, OC5 & OC6. *Remote Sens. Environ.* **2019**, *229*, 32–47. [[CrossRef](#)]
37. Hieronymi, M.; Hereon, H.-Z.; Müller, D.; Krasemann, H.; Brockmann, C.; Ruescas, A.; Stelzer, K.; Bouchra, N.; Ruddick, K.; Simis, S.; et al. *Ocean Colour Remote Sensing of Extreme Case-2 Waters Case 2 eXtreme View Project Space based Cyanobacteria Information & Service (CyanoAlert) View Project Ocean Colour Remote Sensing of Extreme Case-2 Waters*; European Space Agency, Special Publication: Amsterdam, The Netherlands, 2016.
38. Doerffer, R.; Fischer, J. Concentrations of chlorophyll, suspended matter, and gelbstoff in case II waters derived from satellite coastal zone color scanner data with inverse modeling methods. *J. Geophys. Res. Ocean.* **1994**, *99*, 7457–7466. [[CrossRef](#)]
39. Malahlela, O.E.; Oliphant, T.; Tsoeleng, L.T.; Mhangara, P. Mapping chlorophyll-a concentrations in a cyanobacteria-and algae-impacted Vaal Dam using Landsat 8 OLI data. *S. Afr. J. Sci.* **2018**, *114*, 1–9. [[CrossRef](#)]
40. Balasubramanian, S.V.; Pahlevan, N.; Smith, B.; Binding, C.; Schalles, J.; Loisel, H.; Gurlin, D.; Greb, S.; Alikas, K.; Randla, M. Robust algorithm for estimating total suspended solids (TSS) in inland and nearshore coastal waters. *Remote Sens. Environ.* **2020**, *246*, 111768. [[CrossRef](#)]
41. Gitelson, A.A.; Schalles, J.F.; Hladik, C.M. Remote chlorophyll-a retrieval in turbid, productive estuaries: Chesapeake Bay case study. *Remote Sens. Environ.* **2007**, *109*, 464–472. [[CrossRef](#)]
42. Gons, H.J.; Rijkeboer, M.; Ruddick, K.G. A chlorophyll-retrieval algorithm for satellite imagery (Medium Resolution Imaging Spectrometer) of inland and coastal waters. *J. Plankton Res.* **2002**, *24*, 947–951. [[CrossRef](#)]
43. Gons, H.J. Optical teledetection of chlorophyll a in turbid inland waters. *Environ. Sci. Technol.* **1999**, *33*, 1127–1132. [[CrossRef](#)]
44. Pahlevan, N.; Roger, J.-C.; Ahmad, Z. Revisiting short-wave-infrared (SWIR) bands for atmospheric correction in coastal waters. *Opt. Express* **2017**, *25*, 6015–6035. [[CrossRef](#)]
45. Abiye, T.A. Provenance of groundwater in the crystalline aquifer of Johannesburg area, South Africa. *Int. J. Phys. Sci.* **2011**, *6*, 98–111.
46. De Villiers, C.J.; Barnard, P. Environmental reporting in South Africa from 1994 to 1999: A research note. *Meditari Account. Res.* **2000**, *8*, 15–23. [[CrossRef](#)]
47. The Department of Water Affairs and Forestry (DWAF). *Crocodile (West) River Catchment: Internal Strategic Perspective*; Department of Water Affairs and Forestry: Pretoria, South Africa, 2004.
48. The Department of Water Affairs and Forestry (DWAF). *Hartbeespoort Dam Integrated Biological Remediation Program*; Department of Water Affairs and Forestry: Pretoria, South Africa, 2007; pp. 1–18.
49. Kerrigan, K.; Ali, K.A. Application of Landsat 8 OLI for monitoring the coastal waters of the US Virgin Islands. *Int. J. Remote Sens.* **2020**, *41*, 5743–5769. [[CrossRef](#)]
50. Pahlevan, N.; Sarkar, S.; Franz, B.A.; Balasubramanian, S.V.; He, J. Sentinel-2 MultiSpectral Instrument (MSI) data processing for aquatic science applications: Demonstrations and validations. *Remote Sens. Environ.* **2017**, *201*, 47–56. [[CrossRef](#)]
51. Franz, B.A.; Werdell, P.J. A Generalized Framework for Modeling of Inherent Optical Properties in Remote Sensing Applications. In Proceedings of the Ocean Optics, Anchorage, AK, USA, 25 September–1 October 2010.
52. Shi, W.; Wang, M. Detection of turbid waters and absorbing aerosols for the MODIS ocean color data processing. *Remote Sens. Environ.* **2007**, *110*, 149–161. [[CrossRef](#)]
53. Shi, W.; Wang, M.; Zhang, Y. Inherent optical properties in lake taihu derived from VIIRS satellite observations. *Remote Sens.* **2019**, *11*, 1426. [[CrossRef](#)]
54. Carswell, T.; Costa, M.; Young, E.; Komick, N.; Gower, J.; Sweeting, R. Evaluation of MODIS-Aqua atmospheric correction and chlorophyll products of Western North American coastal waters based on 13 years of data. *Remote Sens.* **2017**, *9*, 1063. [[CrossRef](#)]
55. Wang, M.; Shi, W.; Jiang, L. Atmospheric correction using near-infrared bands for satellite ocean color data processing in the turbid western Pacific region. *Opt. Express* **2012**, *20*, 741–753. [[CrossRef](#)]
56. Wang, D.; Ronghua, M.; Xue, K.; Li, J. Improved atmospheric correction algorithm for Landsat 8—OLI data in turbid waters: A case study for the Lake Taihu, China. *Opt. Express* **2019**, *27*, A1400. [[CrossRef](#)]
57. DWAF. *South African Water Quality Guidelines—Domestic Water Use*, 2nd ed.; Department of Water Affairs and Forestry: Pretoria, South Africa, 1996; Volume 1, pp. 86–87.
58. Abiye, T.A.; Leketa, K.C. Historic Climatic Variability and Change: The Importance of Managing Holocene and Late Pleistocene Groundwater in the Limpopo River Basin, Southern Africa. In *Climate Change and Water Resources in Africa*; Springer: Berlin/Heidelberg, Germany, 2021; pp. 131–143.
59. Welch, E.B.; Cooke, G.D. Internal phosphorus loading in shallow lakes: Importance and control. *Lake Reserv. Manag.* **2005**, *21*, 209–217. [[CrossRef](#)]
60. Mulholland, P.G.; Ronnie Best, G.; Coutant, C.C.; Hornberger, G.M.; Meyer, J.L.; Robinson, P.J.; Stenberg, J.R.; Eugene Turner, R.; Vera-Herrera, F.; Wetzel, R.G. Effects of climate change on freshwater ecosystems of the south-eastern United States and the Gulf Coast of Mexico. *Hydrol. Process.* **1997**, *11*, 949–970. [[CrossRef](#)]
61. Lürling, M.; Eshetu, F.; Faassen, E.J.; Kosten, S.; Huszar, V.L.M. Comparison of cyanobacterial and green algal growth rates at different temperatures. *Freshw. Biol.* **2013**, *58*, 552–559. [[CrossRef](#)]